

## **LOADED MICROSTRIP DISK RESONATOR EXHIBITS ULTRA-LOW FREQUENCY RESONANCE**

**T. Chakravarty**

SAMEER, Plot-L2, Block-GP, Sector-5  
Salt Lake, Kolkata-700091, India

**S. M. Roy**

Department of Electronics & Telecommunication Engineering  
Bengal Engineering College  
Shibpur, Howrah-711103, India

**S. K. Sanyal**

Department of Electronics & Telecommunication Engineering  
Jadavpur University  
Kolkata-700032, India

**A. De**

Department of Electronics & Communication Engineering  
Delhi College of Engineering  
Sahabad, Bawana Road, Delhi-110042, India

**Abstract**—In this paper a novel method of generation of ultra-low resonance in a microstrip disk resonator is presented. The disk resonator is loaded with series L-C circuit across a selective location in the disk via a thin shorting pin. It is shown that in loaded disk resonator, the lowest resonance observed is in VHF range whereas the unloaded disk had a fundamental resonance at 1.76 GHz. This resonance is slightly offset from the series resonant frequency of L-C circuit. and it depends on the disk radius as well. Using IE3D, a commercial MoM solver, the said structure is simulated. The experimental results agree well with the simulated results. A closed form expression for computing the resonant frequency is given.

**1 Introduction****2 Theory****3 Simulation and Experimental Results****4 Conclusion****References****1. INTRODUCTION**

Modern communication systems often require compact antenna. Microstrip structures loaded with shorting pins, varactor diodes etc often lead to the practical realizability of such antenna. Loading can take various forms such as stub loading, slots, shorting posts, parasitic couplings, substrate loading, superstrate cover, resistors, capacitors and diodes. An excellent overview of loaded microstrip structures is given by Garg et al. [1]. In a recent work Majumdar et al. [2] have demonstrated the feasibility of tunable compact antenna driven by computer interface. The said circular microstrip antenna is suitably loaded with shorting pin and varactor diodes. Chakravarty et al. [3] have theoretically analyzed such structure. It is shown that the varactor diode's parasitic elements play a key role in generation of ultra-low resonant frequency for the loaded structure as compared to the unloaded case. In this article, the same idea is enhanced to generate a still lower frequency resonance utilizing a suitable combination of inductance and capacitance as loads. The unloaded disk resonator used for analysis has the lowest resonant frequency corresponding to  $TM_{11}$  mode of operation at 1.76 GHz. It is then shown that suitably loading the structure by a combination of shorting post, inductance and capacitance, the lowest resonant mode of operation can be reduced to VHF range of 70–120 MHz. This corresponds to  $TM_{01}$  mode, which is static in the unloaded case.

The structure is simulated using IE3D, a commercial MoM solver. It is seen from the simulated radiation pattern that the theoretical prediction is accurate.

**2. THEORY**

The geometry of the loaded microstrip disk resonator is shown in Fig. 1. The probe fed disk of radius  $r_1$  is loaded at a certain radial location  $r_2$ . The load (inductance  $L_s$  and capacitance  $C_s$  in series) is connected to the patch through a thin metallic pin of radius  $\Delta$ . For the case

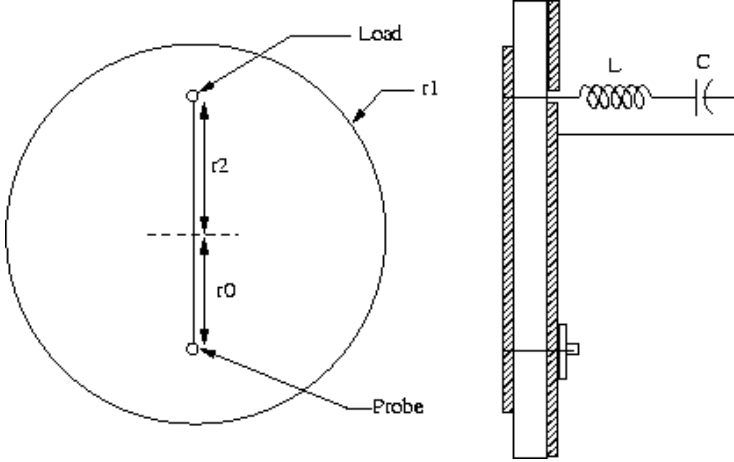


**Figure 1.** Geometry of loaded microstrip disk resonator.

of a probe-fed circular patch, this configuration may be assumed to be a series L-C circuit loading a parallel RLC circuit. We assume that the inductive post along with series L-C load divides the patch into two concentric circles namely region I ( $0 < r < r_2$ ) and region II ( $r_2 < r < r_1$ )

For region I ( $r_2 > r > 0$ ), the expressions for electric and magnetic fields are obtained as

$$E_z^{(1)} = -j\omega_{np}\mu\{C_1 J_n(k_{np}r)\} \cos n\phi \quad (1)$$

$$H_r^{(1)} = -(n/r)\{C_1 J_n(k_{np}r)\} \sin n\phi \quad (2)$$

and

$$H_\phi^{(1)} = -k_{np}\{C_1 J'_n(k_{np}r)\} \cos n\phi \quad (3)$$

where  $J_n(X)$  is Bessel function of first kind of order  $n$ ,  $\omega_{np}$  and  $k_{np}$  are the angular frequency and propagation constant for  $TM_{np}$  mode and  $C_1$  is a constant. Prime denotes a derivative with respect to its argument. The integer ' $n$ ' corresponds to the order of the Bessel function and ' $p$ ' denotes the  $p$ th zero of  $J'_n(k_{np}r)$ . The subscript ' $z$ ' is ignored for particular mode identification as the electric field is non variant along  $z$  direction.

Similarly for region II ( $r_1 > r > r_2$ ), the expressions for electric and magnetic fields are obtained as

$$E_z^{(2)} = -j\omega_{np}\mu\{C_2 J_n(k_{np}r) + C_3 N_n(k_{np}r)\} \cos n\phi \quad (4)$$

$$H_r^{(2)} = -(n/r)\{C_2 J_n(k_{np}r) + C_3 N_n(k_{np}r)\} \sin n\phi \quad (5)$$

and

$$H_{\phi}^{(2)} = -k_{np}\{C_2 J'_n(k_{np}r) + C_3 N'_n(k_{np}r)\} \cos n\phi \quad (6)$$

where  $N_n(X)$  is bessel function of second kind.

It is assumed that the diameter of the circular metallic post connecting the load to the patch is small. Such a thin post is assumed to be replaced by a conductor in the form of a circular arc strip having arc length equal to diameter of the post coincidence with a circle of radius  $r_2$ . For arc strip of small arc length the axial current may be assumed to be uniform along its width. This current is given as  $E_z/Z_0$  where  $Z_0$  is the impedance per unit length for the post. The impedance of such a post is given as (4)

$$Z_0 = \frac{\eta k}{4} \left[ 1 - J_0^2(kr_2) + j \left\{ \frac{2}{\pi} \ln \left( \frac{2}{\gamma k \Delta} \right) + J_0(kr_2) N_0(kr_2) \right\} CF \right] \quad (7)$$

where CF designates a correction factor given as

$$CF = \frac{\sin \left( \frac{\pi}{2\varepsilon_n} \right) \left\{ J_0 \left( \frac{P}{4\varepsilon_n} \right) \right\}^{2P}}{J_0^{1.3}(\alpha_n td) J_0^{1.8}(td)} \quad (8)$$

The disk radiator structure can be seen to be loaded with two reactances namely the post inductance  $L_p$  and the load reactance  $Z_d$ . These two reactive components are placed in series to each other and can be considered to be loading the disk resonator in shunt.

The total impedance can be written as

$$Z_T = j\omega \left\{ \frac{\mu}{2\pi} \left[ \ln \left( \frac{2}{\gamma k \Delta} \right) + \frac{\pi}{2} J_0(kr_2) N_0(kr_2) \right] CF + L_s - \frac{1}{\omega^2 C_s} \right\} \quad (9)$$

The electric and magnetic fields given by Eqns. (1)–(6) satisfy the following boundary conditions.

$$E_z^{(2)} = E_z^{(1)} \quad \text{at } r = r_2 \quad (10)$$

$$H_{\phi}^{(2)} = 0 \quad \text{at } r = r_1 \quad (11)$$

$$H_{\phi}^{(2)} - H_{\phi}^{(1)} = E_z^{(2)} / (Z_T \cdot 2\Delta) \quad \text{at } r = r_2$$

$$\text{for } \phi_i - \alpha/2 < \phi < \phi_i + \alpha/2 \quad (12)$$

where  $\alpha$  is the angle subtended by post at the centre of patch and we assume that complex wall impedance for the thin patch is negligibly small.

Using the boundary conditions given by Eqs. (10) and (11) the expressions for the fields in region II can be re-written as

$$E_z^{(2)} = -j\omega_{np}\mu C_n^{(2)} F_n^{(2)}(k_{np}r) \cos n\phi \quad (13)$$

$$H_r^{(2)} = -(n/r)C_n^{(2)} F_n^{(2)}(k_{np}r) \sin n\phi \quad (14)$$

and

$$H_\phi^{(2)} = -k_{np}C_n^{(2)} F_n^{(2)'}(k_{np}r) \cos n\phi \quad (15)$$

where

$$\begin{aligned} C_n^{(2)} &= C_2/N_n'(k_{np}r_1) \\ F_n^{(2)}(k_{np}r) &= [J_n(k_{np}r)N_n'(k_{np}r_1) - J_n'(k_{np}r_1)N_n(k_{np}r)] \\ F_n^{(2)'}(k_{np}r) &= [J_n'(k_{np}r)N_n'(k_{np}r_1) - J_n'(k_{np}r_1)N_n'(k_{np}r)] \end{aligned}$$

similarly fields in region I can be written in terms of  $C_n^{(1)}$ ,  $F_n^{(1)}(k_{np}r)$ ,  $F_n^{(1)'}(k_{np}r)$

$$E_z^{(1)} = -j\omega_{np}\mu C_n^{(1)} F_n^{(1)}(k_{np}r) \cos n\phi \quad (16)$$

$$H_r^{(1)} = -(n/r)C_n^{(1)} F_n^{(1)}(k_{np}r) \sin n\phi \quad (17)$$

and

$$H_\phi^{(1)} = -k_{np}C_n^{(1)} F_n^{(1)'}(k_{np}r) \cos n\phi \quad (18)$$

where

$$\begin{aligned} C_n^{(1)} &= C_1 \\ F_n^{(1)}(k_{np}r) &= J_n(k_{np}r) \end{aligned}$$

and

$$F_n^{(1)'}(k_{np}r) = J_n'(k_{np}r)$$

Applying boundary conditions given by Eqns. (10), (12) two homogenous equations in  $C_n^{(1)}$  and  $C_n^{(2)}$  are obtained. For  $C_n^{(1)}$  and  $C_n^{(2)}$  to be non vanishing the determinant of the equations so derived should be zero, which leads to

$$\frac{F_n^{(2)'}(tx)}{F_n^{(2)}(tx)} - \frac{F_n^{(1)'}(tx)}{F_n^{(1)}(tx)} - \frac{\varepsilon_n(1 + \cos(2n\phi_i))}{2txX_T} = 0 \quad (19)$$

where

$$X_T = \left\{ \ln \left( \frac{2t_2}{\gamma x} \right) + \frac{\pi}{2} J_0(tx) N_0(tx) \right\} CF + \left( L_s - \frac{1}{\omega^2 C_s} \right) \frac{2\pi}{\mu_0} \quad (20)$$

where  $t = r_2/r_1$ ;  $T = \sin(n\alpha)/n\alpha$ ;  $x = k_{np}r_1$  and  $\varepsilon_n = 1$  for  $n = 0$ ,  $\varepsilon_n = 2$  for  $n \neq 0$ .

The resonance frequency for a given mode ‘ $np$ ’ is obtained by solving Eq. (19) where integer ‘ $n$ ’ denotes the order of Bessel’s function and ‘ $p$ ’ corresponds to the  $p$ th zero of Eq. (19).

In the present case, the dimensions are as follows:  $r_1$  (radius of disk resonator) = 33.1 mm,  $r_2$  (radial location of load) = 28 mm,  $h$  (height of the substrate) = 0.79 mm,  $\varepsilon_r = 2.2$ ,  $\Delta$  (radius of post) = 0.15 mm,  $r_0$  (feed probe location) = 16 mm. In a microstrip disk of radius  $r_1$ , the load comprising of inductance  $L_s = 220$  nH/330 nH and a trimmer capacitance = 10 pf–33 pf is connected to the disk at radial location of  $r_2$ ,  $\varphi_i$  via a thin post of radius  $\Delta$ . Here  $\varphi_i = 180^\circ$ , the angle between the feed probe and the load. It is seen from the solution of (1) that a lower frequency resonance corresponding to  $TM_{01}$  mode is generated. The higher order modes remain unchanged from their unloaded resonances.

### 3. SIMULATION AND EXPERIMENTAL RESULTS

The said structure is simulated and fabricated as well. The resonant frequencies are experimentally measured using HP8757D Scalar Network Analyzer. There is excellent agreement between theory, measurements & simulation. It is seen experimentally that as the capacitance value is changed from 10 pf to 33 pf, the lowest resonant frequency is tuned from 114 MHz to 71 MHz (60 MHz for  $L_s = 330$  nH). However measured results show that the input return loss seen by the feed probe for a fixed probe location is not better than  $-10$  dB throughout the tuning range. Thus the utility of such structure as matched antenna is limited over the frequency range. Moreover, being electrically thin this structure is a weak radiator. Fig. 2 shows a comparison between simulated and theoretical prediction for different patch radii. As the patch radius is increased the resonant frequency is decreased till it reaches the series resonant frequency of the individual L-C circuit. In Fig. 3, the change in resonance due to variable capacitor values is shown. In Fig. 4 the simulated return loss for different capacitor values is shown. It is seen that the structure does not reflect a VSWR better than 2:1 over the whole frequency range. In Fig. 5 and 6, the simulated resonant frequencies as well as the return loss at resonance is displayed for different load and probe locations respectively. It is seen that the change in resonant frequency with load location is marginal, whereas the change in input matching depends strongly on probe location.

In Fig. 7, the measured return loss for two values of capacitance

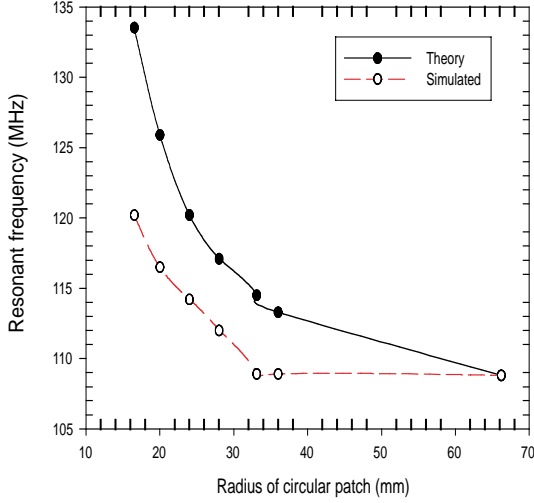


**Figure 2.** Comparison between theoretical prediction and simulated resonant frequencies for the loaded circular patch for different patch radii. ( $r_2/r_1 = 0.85$ ,  $h = 0.79$  mm,  $\Delta = 0.15$  mm,  $\epsilon_r = 2.2$ ,  $L_s = 220$  nH,  $C = 10$  pf).

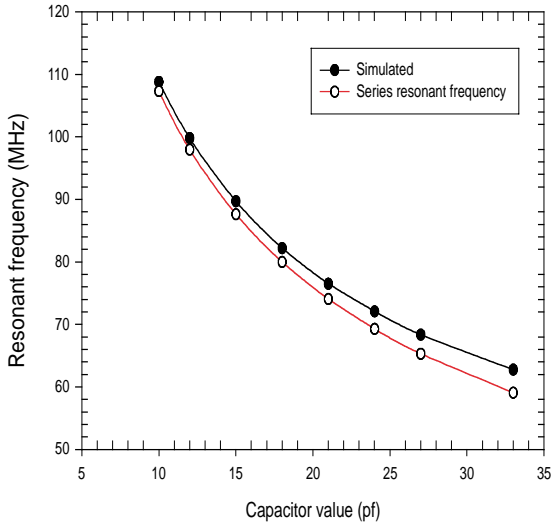


**Figure 3.** Simulated resonant frequencies for the loaded circular patch for different load capacitor values. ( $r_1 = 33.1$  mm,  $r_2 = 28$  mm,  $h = 0.79$  mm,  $\Delta = 0.15$  mm,  $\epsilon_r = 2.2$ ,  $L_s = 220$  nH).

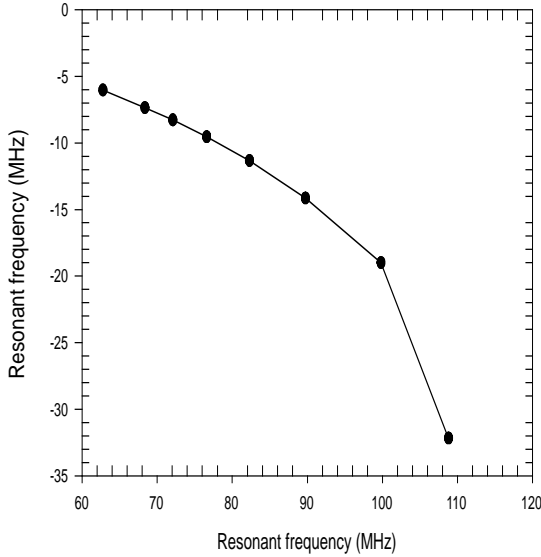


**Figure 4.** Simulated return loss at resonance for the loaded circular patch for different capacitor values at resonance. ( $r_1 = 33.1$  mm,  $r_2 = 28$  mm,  $h = 0.79$  mm,  $\Delta = 0.15$  mm,  $\epsilon_r = 2.2$ ,  $L_s = 220$  nH).

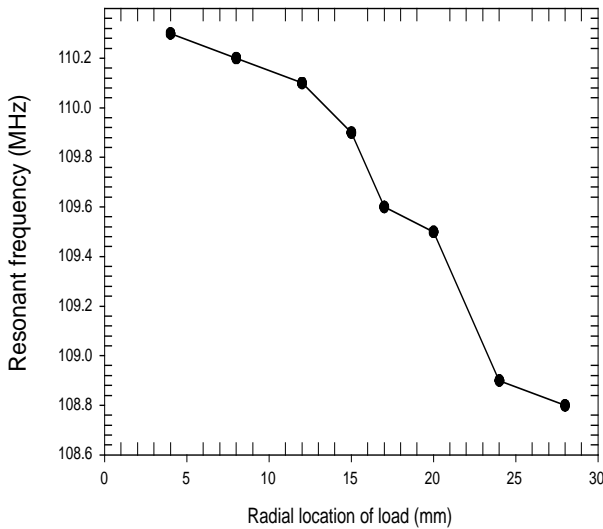


**Figure 5.** Simulated frequency for the loaded circular patch for different load locations  $r_2$ . ( $r_1 = 33.1$  mm,  $h = 0.79$  mm,  $\Delta = 0.15$  mm,  $\epsilon_r = 2.2$ ,  $L_s = 220$  nH,  $C = 10$  pf).

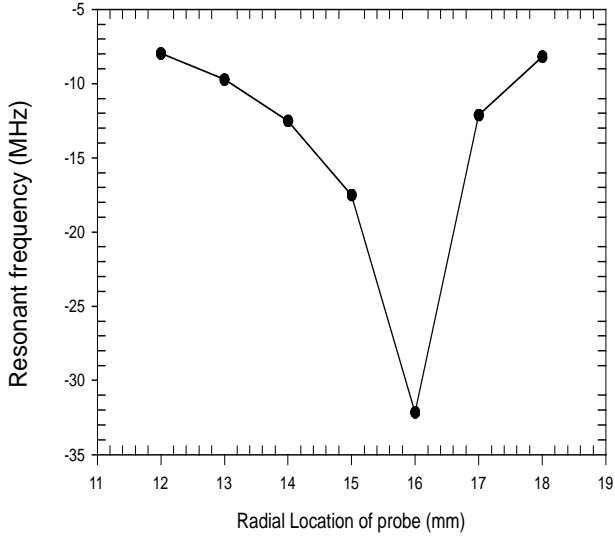


**Figure 6.** Simulated return loss for the loaded circular patch for different probe locations  $r_0$ . ( $r_1 = 33.1$  mm,  $r_2 = 28$  mm,  $h = 0.79$  mm,  $\Delta = 0.15$  mm,  $\epsilon_r = 2.2$ ,  $L_s = 220$  nH,  $C = 10$  pf).

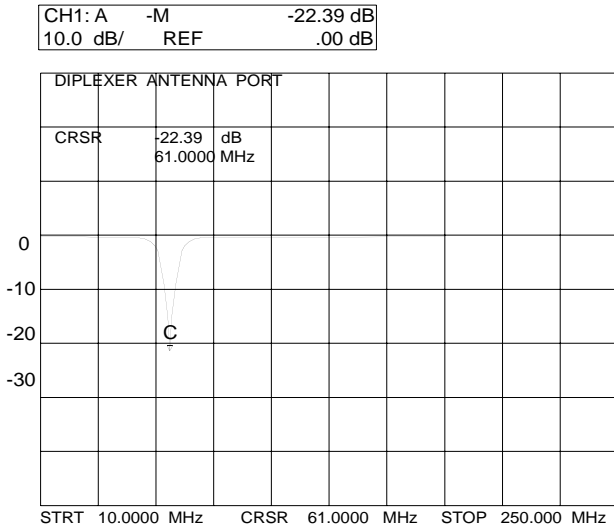


**Figure 7.** Measured return loss for the loaded circular patch for different values of load impedance. ( $r_1 = 33.1$  mm,  $r_2 = 28$  mm,  $h = 1.59$  mm,  $\Delta = 0.15$  mm,  $\epsilon_r = 2.2$ ,  $L_s = 330$  nH).

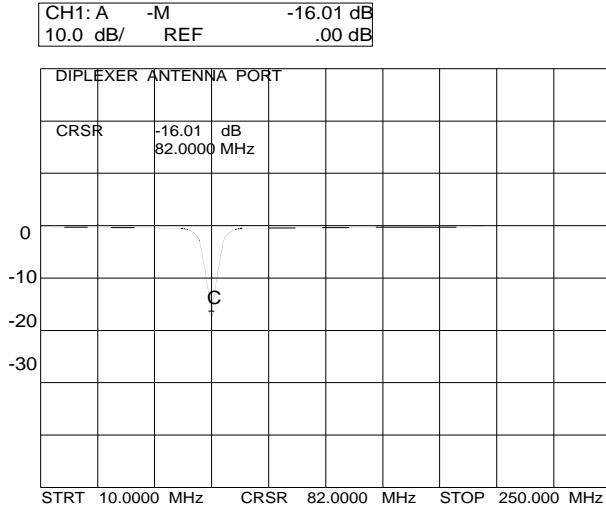


**Figure 8.** Measured return loss for the loaded circular patch. ( $r_1 = 33.1$  mm,  $r_2 = 28$  mm,  $h = 1.59$  mm,  $\Delta = 0.15$  mm,  $\epsilon_r = 2.2$ ,  $L_s = 330$  nH,  $C = 10$  pf).

are presented. It is clearly seen that the resonant frequency as well as the return loss changes with different values of load impedance. A close snapshot of the measured return loss is presented in Fig. 8 to display the  $Q$  factor of the resonance from one-port measurement. The estimated  $Q$  of the resonance is of the order of 25 with bandwidth measured at 2:1 VSWR.

#### 4. CONCLUSION

The mode of operation for the lowest resonance in the loaded disk is  $TM_{01}$ . Therefore the beam pattern will display a null in the broadside direction with azimuth symmetry. Since the radiator is operating in  $TM_{01}$  mode, it is expected that far field radiation pattern will exhibit a null in the boresight with azimuth symmetry making it useful for angle of arrival determination if operated in elevation or as a monopole antenna if operated in azimuth. Since the antenna efficiency is likely to be extremely low such radiation measurements are not found useful for practical purposes. However with increase in antenna efficiency by increasing the height of substrate (air dielectric), the far field measurements can be done. Studies on these are continuing.

Therefore, such structure can possibly be utilized as indoor antenna with a  $360^\circ$  azimuth coverage. The efficiency of such antenna

is likely to be low. The efficiency can be enhanced by increasing the height of the substrate. The given structure is expected to be poor radiator with efficiency less than 1 increased if the height is increased to 10mm. For such cases the antenna efficiency rises to 48% with increase in bandwidth in the VHF range. Simulation studies on these aspects are continuing.

A number of variations in such loading technique can be incorporated thereby resulting in sharply tuned bandpass filter, broadband microstrip antenna in VHF range etc. Replacing the trimmer capacitor with an equivalent varactor diode, one can digitally tune the loaded structure leading to a frequency hopping antenna. In conclusion, we have presented a method of generation of ultra-low resonance from a normally L-band resonating structure.

## REFERENCES

1. Garg, R., P. Bhartia, I. Bahl, and A. Ittipiboon, *Microstrip Antenna Design Handbook*, Artech House, Norwood, MA, 2000.
2. Majumdar, A., T. Chakravarty, S. Saran, and S. K. Sanyal, "A novel technique to implement frequency hopping planar antennas with a computer interface," *Microw. and Optical Tech. Letters*, Vol. 38, 270–274, August 20, 2003.
3. Chakravarty, T., S. K. Sanyal, and A. De, "Compact and tunable circular microstrip patch using post-varactor loading," *IETE Tech Review*, Vol. 18, 153–157, 2001.
4. Chakravarty, T. and A. De, "Resonant frequency of a shorted circular patch with the use of a modified impedance expression for a metallic post," *Microw. and Optical Tech. Letters*, Vol. 33, No. 4, 252–256, May 20, 2002.

**Tapas Chakravarty** obtained M.Sc. (Electronics Science) from Delhi University in 1998. He worked as Scientific Officer in SAMEER Mumbai from 1988 to 1993. There he participated in development of MST radar at Gadanki. From 1993 he has continued in SAMEER — Kolkata. His present interests include Microwave passive circuits and Microstrip Antenna.

**Sushim Mukul Roy** did his Bachelor of Engineering in Electronics and Telecommunication from Bengal Engineering College, Shibpur (India) in the year 2003. Presently he is working as a Process Engineer in Samtel Color Ltd., Ghaziabad, India. His research interests are Microstrip Antennas and Microwave Passive circuits.

**Salil Kumar Sanyal** obtained his M.E.Tel.E. and Ph.D. (Engg.) degrees from Jadavpur University, Kolkata, India in 1979 and 1990 respectively. He joined the Department of Electronics and Telecommunication Engineering, Jadavpur University as Lecturer in 1982 and currently he is Reader at the same Department. His research interests include programmable microstrip antenna, signal processing and communication systems. He is a Senior Member of IEEE (USA).

**Ashok De** obtained his M.E. (E & TCE) from Jadavpur University, Calcutta in 1980 followed by Ph.D. from IIT Kharagpur in 1985. He joined Dept. of Electronics Science of Delhi University as Lecturer in 1985 and continued till 1991 when he joined Calcutta University as Reader. Presently he is Professor in Delhi Engineering College. His research interest includes microstrip antennas.